Journal of Bacteriology

Differential Regulation of High-Affinity Phosphate Transport Systems of *Mycobacterium smegmatis*: Identification of PhnF, a Repressor of the *phnDCE* Operon

Susanne Gebhard and Gregory M. Cook
J. Bacteriol. **2008, 190(4):1335. DOI: 10.1128/JB.01764-07.**
Published Ahead of Print 14 December 2007.

JOURNAL OF BACTERIOLOGY, Feb. 2008, p. 1335–1343 Vol. 190, No. 4
0021-9193/08/$08.00+0 doi:10.1128/JB.01764-07

Differential Regulation of High-Affinity Phosphate Transport Systems of *Mycobacterium smegmatis*: Identification of PhnF, a Repressor of the *phnDCE* Operon[▽]

Susanne Gebhard and Gregory M. Cook*

Department of Microbiology and Immunology, Otago School of Medical Sciences, University of Otago, P.O. Box 56, Dunedin, New Zealand

Received 6 November 2007/Accepted 6 December 2007

The uptake of phosphate into the cell via high-affinity, phosphate-specific transport systems has been studied with several species of mycobacteria. All of these species have been shown to contain several copies of such transport systems, which are synthesized in response to phosphate limitation. However, the mechanisms leading to the expression of the genes encoding these transporters have not been studied. This study reports on the investigation of the regulation of the *pstSCAB* and the *phnDCE* operons of *Mycobacterium smegmatis*. The *phn* locus contains an additional gene, *phnF*, encoding a GntR-like transcriptional regulator. Expression analyses of a *phnF* deletion mutant demonstrated that PhnF acts as a repressor of the *phnDCE* operon but does not affect the expression of *pstSCAB*. The deletion of *pstS*, which is thought to cause the constitutive expression of genes regulated by the two-component system SenX3-RegX3, led to the constitutive expression of the transcriptional fusions *pstS-lacZ*, *phnD-lacZ*, and *phnF-lacZ*, suggesting that *phnDCE* and *phnF* are conceivably new members of the SenX3-RegX3 regulon of *M. smegmatis*. Two presumptive binding sites for PhnF in the intergenic region between *phnD* and *phnF* were identified and shown to be required for the repression of *phnD* and *phnF*, respectively. We propose a model in which the transcription of *pstSCAB* is controlled by the two-component SenX3-RegX3 system, while *phnDCE* and *phnF* are subject to dual control by SenX3-RegX3 and PhnF.

Phosphorus is an essential nutrient for all cells and is required for energy metabolism and for the synthesis of important biological molecules such as phospholipids and nucleic acids. The main source of phosphorus for bacteria is inorganic phosphate. To ensure the supply of phosphorus under conditions of phosphate limitation, bacteria possess a high-affinity phosphate-specific ABC transport system (Pst), and some species contain additional systems for the utilization of alternative phosphorous sources, such as phosphite (e.g., as in the Ptx system of *Pseudomonas stutzeri*) (22) or phosphonates (e.g., as in the Phn system of *Escherichia coli*) (20, 37). In the slow-growing pathogenic species of mycobacteria, multiple copies of the genes encoding the Pst system have been identified (17), and two of these genes, *pstS1* and *pstS2*, were shown to be important for the virulence of *Mycobacterium tuberculosis* (25). We recently showed that the fast-growing *M. smegmatis* also requires several high-affinity phosphate-specific transport systems for growth (5), suggesting that this is a general characteristic of mycobacteria. The reasons for the presence of multiples of such transporters are not well understood, but this characteristic has been proposed to constitute an adaptation of the bacteria to grow and survive in a variety of phosphate-limited environments (17). If this is the case, it appears likely that the expression of multiple high-affinity phosphate transport systems in mycobacteria should be regulated differentially.

Transcription of the genes for bacterial high-affinity phosphate transport systems is usually regulated by a two-component regulatory system, PhoBR in gram-negative bacteria (37) and PhoPR in gram-positive bacteria (13, 33), where PhoR acts as the sensor kinase and PhoB or PhoP acts as the cognate response regulator. Additionally, the Pst system and the repressor PhoU are required for signal transduction and, together with PhoR, are thought to form a membrane-bound repressor complex under phosphate-replete conditions (37). Mutations in Pst have been shown to lead to constitutive activation of the Pho regulon genes in a number of bacteria such as *E. coli* (39), *Sinorhizobium meliloti* (41), and *M. smegmatis* (15).

Recently, the sensor kinase SenX3 and the response regulator RegX3 were identified as composing the phosphate-responsive two-component regulatory system of *M. smegmatis* (6). RegX3 was shown to bind to the promoters of several genes, including *pstS*, the first gene of the operon that encodes the Pst transport system (6). The authors proposed that SenX3 is unlikely to sense the phosphate availability in the medium directly but probably relies on the Pst transporter to relay this information and thus regulate the activity of SenX3, similar to the situation in *E. coli* (6). While putative RegX3 binding sites were identified in the promoter regions of *senX3*, *phoA* (encoding alkaline phosphatase), and *pstS*, the sequence conservation between these regions was too weak to predict which other genes might be controlled by SenX3-RegX3 (6).

As stated above, we recently identified a second high-affinity phosphate ABC transport system of *M. smegmatis*, the PhnDCE system, which has a sequence similarity to the phos-

* Corresponding author. Mailing address: Department of Microbiology and Immunology, Otago School of Medical Sciences, University of Otago, P.O. Box 56, Dunedin, New Zealand. Phone: 64 3 479 7722. Fax: 64 3 479 8540. E-mail: greg.cook@stonebow.otago.ac.nz.

▽ Published ahead of print on 14 December 2007.

TABLE 1. Bacterial strains and plasmids used in this study

Bacterial strain or plasmid	Description[a]	Source or reference
Strains		
E. coli		
DH10B	F$^-$ *mcrA* Δ(*mrr-hsdRMS-mcrBC*) ϕ80d*lacZ* ΔM15 Δ*lacX74 deoR recA1 araD139* Δ(*ara leu*)*7697 galU galK rpsL endA1 nupG*	10
M. smegmatis		
mc^{2}155	Electrocompetent wild-type strain of *M. smegmatis*	32
SG62	mc^{2}155 Δ*phnF*::*aphA-3*; Km^r	This study
SG95	mc^{2}155 Δ*pstS*::*aacC-1*; Gm^r	5
SG111	SG62 with pSG41 integrated in *attB*; Km^r Hyg^r	This study
SG120	SG95 with pSG43 integrated in *attB*; Gm^r Hyg^r	5
Plasmids		
pBluescript II KS	Cloning vector; Ap^r	Stratagene
pUC18K	*E. coli* plasmid containing an excisable, nonpolar kanamycin resistance cassette; Km^r Ap^r	19
pX33	*E. coli*-mycobacterium shuttle vector for allelic exchange mutagenesis in mycobacteria, pPR23, carrying a constitutive *xylE* marker; Gm^r Sac^s ts	5, 26
pJEM15	*E. coli*-mycobacterium shuttle vector for the creation of transcriptional promoter fusions to *lacZ*; Km^r	34
pUHA267	*E. coli* vector with mycobacteriophage L5 integrase and *attP* for integration into *attB* of mycobacteria; Hyg^r	AgResearch, Wallaceville, New Zealand
pSG10	pJEM15 harboring a 500-bp *phnD-lacZ* fusion; Km^r	5
pSG16	pX33 harboring Δ*phnF*::*aphA-3*; Km^r Gm^r Sac^s ts	This study
pSG18	pJEM15 harboring a 500-bp *phnF-lacZ* fusion	This study
pSG41	pUHA267 harboring *phnF*$^+$ with its native promoter; Hyg^r	This study
pSG42	pJEM15 harboring a 560-bp *pstS-lacZ* fusion; Km^r	5
pSG43	pUHA267 harboring *pstS*$^+$ with its native promoter; Hyg^r	5

[a] Gm^r, gentamicin resistance; Hyg^r, hygromycin resistance; Ap^r, ampicillin resistance; Sac^s, sucrose sensitivity; ts, temperature sensitivity.

phonate/phosphite transporters of several gram-negative bacteria such as *E. coli* (21), *P. stutzeri* (40), and *S. meliloti* (3) but appears to be specific for phosphate and not phosphonate or phosphite in *M. smegmatis* (5). A gene adjacent to but divergently transcribed from the *M. smegmatis phnDCE* operon has been identified as a putative transcriptional regulator of the GntR family and was designated *phnF* (36). The *phn* operon of *E. coli* also contains a *phnF* gene that is proposed to have a role in the regulation of gene expression, but no definite function has been assigned to its gene product (21).

In the present study, we investigated the mechanisms of regulation of the *phnDCE* and the *pstSCAB* operons of *M. smegmatis*. We used allelic exchange mutagenesis and RNA analysis to investigate the role of PhnF in transcriptional regulation of the *phnDCE* and *pstSCAB* operons. We also used a *pstS* deletion mutant to determine whether the *phnDCE* operon is part of the phosphate regulon in *M. smegmatis*. Site-directed mutagenesis of the region between *phnD* and *phnF* revealed two putative binding sites for PhnF in the promoters of *phnDCE* and *phnF*.

MATERIALS AND METHODS

Bacterial strains and growth conditions. All strains and plasmids used in this study are listed in Table 1. *E. coli* strains were grown in Luria-Bertani (LB) medium at 37°C with agitation (200 rpm). The *M. smegmatis* mc^{2}155 strain (32) and derived strains were routinely grown at 37°C with agitation at 200 rpm in LB medium containing 0.05% (wt/vol) Tween 80 (LBT) or in Middlebrook 7H9 medium (Difco) supplemented with 10% albumin-dextrose-catalase enrichment (ADC; Becton Dickinson) and 0.05% (wt/vol) Tween 80. *M. smegmatis* transformants were grown at 28°C for the propagation of temperature-sensitive vectors and at 40°C for allelic exchange mutagenesis. For P_i limitation studies, *M. smegmatis* was grown in modified minimal Sauton's medium. The composition of this medium per liter was 0.5 g $MgSO_4$, 2 g citric acid, 1 g L-asparagine, 0.3 g KCl, 1 g glycerol, 0.5 g Tween 80, 320 μl 0.5 M $FeCl_3$, and 100 μl of 1 M NH_4Cl. The high-phosphate medium contained 100 mM K_2HPO_4. For phosphate starvation experiments, cells were grown in high-phosphate medium to an optical density at 600 nm (OD_{600}) of 0.7 to 1.2, washed twice in sterile 0.85% (wt/vol) saline with 0.05% (wt/vol) Tween 80, resuspended to an OD_{600} of 0.7 in phosphate-free Sauton's medium, and incubated at 37°C with agitation at 200 rpm for 2 h.

Selective media contained kanamycin (50 μg ml^{-1} for *E. coli*; 20 μg ml^{-1} for *M. smegmatis*), gentamicin (20 μg ml^{-1} for *E. coli*; 5 μg ml^{-1} for *M. smegmatis*), or hygromycin (200 μg ml^{-1} for *E. coli*; 50 μg ml^{-1} for *M. smegmatis*). Solid medium contained 1.5% agar.

OD_{600} was measured using culture samples diluted in saline to bring the OD_{600} to below 0.5 when measured in cuvettes of 1-cm length light path in a Jenway 6300 spectrophotometer.

DNA manipulation and cloning of constructs. All molecular biology techniques were carried out according to standard procedures (31). Restriction or DNA-modifying enzymes and other molecular biology reagents were obtained from Roche Diagnostics or New England Biolabs.

Genomic DNA of *M. smegmatis* was isolated by a method modified from that described by Gonzalez-y-Merchand et al. (7). In brief, cells grown on LBT agar were resuspended in 200 μl of lysis buffer (4 M guanidine thiocyanate, 1 mM β-mercaptoethanol, 10 mM EDTA, 0.1% [wt/vol] Tween 80), snap-frozen in dry ice-ethanol, and heated to 65°C for 10 min. Snap-freezing/heating was repeated, and the cells were cooled on ice for 5 min. The aqueous phase was extracted twice with chloroform, and DNA was precipitated by isopropanol. The pellet was washed once in 70% ethanol, air dried, and dissolved in deionized water.

To create a transcriptional fusion of *phnF*, a PCR product encompassing 420 bp of DNA upstream of *phnF* plus 110 bp of its coding region was amplified using the primers PphnFF (5′-AAATTTGGGCCCGCATAGTCGGAGGCCTGGACG-3′) and PphnFR (5′-AAATTTGGTACCGGATCCCCGATGCGCATACC-3′). The product was cloned into the ApaI and Asp718 sites of pJEM15 (34), creating the plasmid pSG18.

To create a construct for the deletion of *phnF*, the kanamycin resistance (Km^r) cassette, encoded by *aphA-3*, was amplified from pUC18K (19) by PCR, using the primers 3′mcspUC (5′-GTTTTCCCAGTCACGACGTT-3′) and 5′mcspUC (5′-

CACACAGGAAACAGCTATGA-3′). The resulting 850-bp product was digested with EcoRI and BamHI. PCR products of approximately 850 bp flanking the *phnF* gene of *M. smegmatis* were amplified by using the primer phnFKO1 (5′-AAATTTACTAGTGGCCTCAGAACCCGACTTGA-3′) with primer phnFKO2 (5′-AAATTTGAATTCGGATCCCCGATGCGCATACC-3′) (left flank) and the primer phnFKO3 (5′-AAATTTGGATCCACGGCCGTCATGCACGCTA AG-3′) with primer phnFKO4 (5′-AAATTTACTAGTCGACGCATCCGAAT GCGCAC-3′) (right flank). The left-flank PCR product was digested with SpeI and EcoRI, and the right-flank PCR product was digested with BamHI and SpeI. Both flanking products and the kanamycin cassette were ligated into the SpeI site of the pBluescript II KS plasmid (Stratagene). The resulting assembly, left flank/Km^r/right flank, was subcloned as an SpeI fragment into pX33 (pPR23 [26] carrying a constitutive *xylE* marker), generating the pSG16 plasmid. The expected double-crossover event would result in a nonpolar deletion-insertion at the *phnF* locus, eliminating 80% of the *phnF* coding sequence in exchange for the kanamycin resistance marker. Allelic replacement of *phnF* was carried out essentially as described by Pelicic et al. (26) and was achieved by growing a culture of *M. smegmatis* carrying pSG16 in Middlebrook 7H9-ADC medium at 28°C with agitation (200 rpm) to an OD_{600} of approximately 0.6 to 0.8, followed by plating onto low-salt LBT plates (2 g NaCl liter^{-1}) containing gentamicin and 10% sucrose at 40°C, selecting for double-crossover events. Replacement of *phnF* with the kanamycin marker created strain SG62 (Δ*phnF*::*aphA-3*). For Southern hybridization analysis, SmaI-digested genomic DNA of the putative mutants was separated on a 1% agarose-Tris-acetate-EDTA gel and transferred onto a nylon membrane (Hybond-N$^+$; Amersham) by vacuum blotting. Probes were labeled by random priming using [α-^{32}P]dCTP (Amersham) and Ready-To-Go DNA-labeling beads (Amersham).

The construct used for complementation of the allelic exchange mutant was cloned into the integrative *E. coli*/mycobacterium shuttle vector pUHA267 (16). A 1.2-kb PCR product encompassing the *phnF* gene plus 428 bp of upstream DNA was amplified by PCR using the primers cphnFF (5′-AAATTTAAGCTT CATAGTCGGAGGCCTGGACG-3′) and cphnFR (5′-AAATTTAAGCTTCA AGAATCCGGTGTTTCCGC-3′) and cloned into the HindIII site of pUHA267, creating the plasmid pSG41.

Site-directed mutagenesis of the putative PhnF binding sites (inverted repeat unit 1 [IRU-1] and IRU-2) was carried out using PCR overlap-extension (11). For the mutagenesis of IRU-1, a 158-bp PCR product was amplified with the primers PphnFR and SDMIRU1-1 (5′-ACGTCTGTGTCTATCACAGCGGAC GGCCGTCTGACGAG-3′), and a 247-bp PCR product was amplified using the primers SDMIRU1-2 (5′-GTCCGCTGTGATAGACACAGACGTATTCGCT TGTTC-3′) and PphnDR (5′-AAATTTGGTACCGCTTGTCGGAGCCCGAA CAG-3′). For the mutagenesis of IRU-2, a 216-bp PCR product was amplified with the primers PphnFR and SDMIRU2-1 (5′-GTGGGGTGTGCTATACCA ACGGGTGCATCTCGGG-3′), and a 189-bp PCR product was amplified by using the primers SDMIRU2-2 (5′-ACCCGTTGGTATAGCACACCCCACAA GGTGTGTGG-3′) and PphnDR. These fragment pairs were then used in overlap-extension PCR, using the primers PphnFR and PphnDR, and the resulting products were digested with Asp718 and cloned into the Asp718 site of pJEM15 (34). The orientation of the insert determined whether the resulting construct represented a *phnD-lacZ* or a *phnF-lacZ* fusion. Mutation of both IRUs simultaneously was achieved by using the fragment containing the changes in IRU-1 as a template for the mutagenesis of IRU-2. A fragment containing the wild-type sequence was amplified by using the primers PphnFR and PphnDR.

RNA extraction and dot blot analysis. For RNA extraction, 5 to 10 ml of broth culture was grown to an OD_{600} of 0.5 to 0.7 in high-phosphate Sauton's medium or was subjected to phosphate starvation as described above. Cells were harvested by centrifugation, resuspended in 1.5 ml GTC buffer (5 M guanidine thiocyanate, 25 mM sodium-citrate [pH 7], 0.05% [wt/vol] Tween 80, 0.05% [wt/vol] Sarkosyl), vortexed for 10 s, pelleted again by centrifugation, and stored at −80°C. Total RNA was extracted using TRIzol reagent (Invitrogen) according to the manufacturer's instructions. Cell lysis was achieved by two cycles of bead beating in a Mini-Beadbeater (Biospec) at 5,000 rpm for 1 min. DNA was removed from the RNA preparation by treatment with 2 U of RNase-free DNase, using a TURBO DNA-free kit (Ambion), according to the manufacturer's instructions. RNA concentrations were determined by using a NanoDrop ND-1000 spectrophotometer. For dot blot analysis, serial fourfold dilutions of RNA samples, from 800 ng to 12.5 ng, were prepared in RNase-free water, and RNA was denatured using glyoxal sample buffer (Cambrex Bio Science, Rockland, ME) according to the manufacturer's instructions. Samples were mixed with 2 volumes of 20× SSC (3 M NaCl, 300 mM sodium citrate, pH 7 [1× SSC is 0.15 M NaCl plus 0.015 M sodium citrate]) and applied to a nylon membrane by vacuum, using a Bio-dot apparatus (Bio-Rad). For use as probes, a 980-bp internal fragment of *phnC* was PCR amplified using the primers phnCintF (5′-GCTCCGAGAAGTGCAAGGGCTGAC-3′) and phnCintR (5′-CGATCA GCGCGGTCGGTACGAAATC-3′), and a 1-kb fragment of *pstC* was amplified using the primers pstSKO-3 and pstSKO-4 (5). Probes were labeled by random priming, using [α-^{32}P]dCTP (Amersham) and Ready-To-Go DNA-labeling beads (Amersham).

Mapping of TSSs. The transcriptional start sites (TSSs) of *phnD* and *phnF* were mapped by 5′ rapid amplification of cDNA ends (RACE), using the components of a 3′/5′ RACE kit (Roche) according to the manufacturer's instructions. First-strand cDNA was synthesized from 4 μg of total RNA isolated from phosphate-starved cells of wild-type *M. smegmatis* with the *phnD*-specific primer phnD-RACE1 (5′-CTTGTCGATCATGGTCTTG-3′) or the *phnF*-specific primer phnF-RACE1 (5′-AATTCTTAGCGTGCATGAC-3′). The resulting cDNA was purified, and a deoxyribosyladenine tail was added by following the kit instructions. Purified deoxyribosyladenine-tailed cDNA was then used as a template for PCR using the oligo(dT) anchor primer and the *phnD*-specific primer phnD-RACE2 (5′-ACGAAGCACACCTTCTTG-3′) or the *phnF*-specific primer phnF-RACE2 (5′-GTTGAGCAGGAACATGGG-3′). The resulting PCR products were gel purified and used as templates for a second PCR using the PCR anchor primer and the nested *phnD*-specific primer phnD-RACE3 (5′-CGAGCCCGTAGGACTGGTAGC-3′) or the *phnF*-specific primer phnF-RACE3 (5′-GTGAAGGCGATCCCACGGCTG-3′). These PCR products were cloned into pGEM-T Easy (Promega) according to the manufacturer's instructions. Three clones containing the correctly sized insert for *phnD* (ca. 400 bp) or *phnF* (ca. 550 bp) were sequenced using the primer phnD-RACE3 or phnF-RACE3, respectively, giving consistent results for each gene.

β-Galactosidase and inorganic phosphate assays. To determine the threshold P_i concentration leading to the induction of *phnF*, cells carrying pSG18 were grown in medium containing 200 μM phosphate. The medium was modified from the standard Sauton's medium used in this study to contain higher concentrations of the carbon source (5 g of glycerol liter^{-1}) and the nitrogen source (4 g L-asparagine liter^{-1}), providing both nutrients in excess. At various time points, 2 ml to 4 ml of the culture was removed to determine the OD_{600}. Cells were then pelleted, and cell pellets and supernatants were stored at −20°C. β-Galactosidase activity for the 0-h time point was determined with cells of the inoculum culture. β-Galactosidase activities were determined as described previously (5) and were expressed as Miller units (MU) (23), calculated as the increase in A_{420} per min per 1 ml of cell suspension used (normalized to an OD_{600} of 1.0) and multiplied by a factor of 1,000. Statistical analyses were performed using a two-tailed, unpaired *t* test. The P_i concentration in the supernatant was determined by inorganic phosphate assay as described previously (24).

DNA and protein sequence analysis. The provisional genome sequence of *M. smegmatis* strain mc^{2}155 was accessed via The Institute for Genomic Research (TIGR) website (http://www.tigr.org; GenBank accession number CP000480). Sequence data for *M. tuberculosis* were obtained from the Institut Pasteur website (http://genolist.pasteur.fr/TubercuList). Protein sequence alignments were carried out using a ClustalW function and the BLOSUM62 matrix of BioEdit (9). Secondary-structure predictions were performed using JPred (4). Promoter areas were searched for conserved motifs, using motif discovery and search tool MEME software, available at the San Diego Supercomputer Center website (http://meme.sdsc.edu/meme/).

RESULTS AND DISCUSSION

Identification of a putative regulator in the *phn* locus of *M. smegmatis*. The PhnDCE phosphate transport system of *M. smegmatis* is encoded by a three-gene operon (Fig. 1A) (5). A gene adjacent to and divergently transcribed from this operon, MSMEG_0650, has been annotated as a GntR family transcriptional regulator encoding a 244-amino-acid protein. According to the results of a conserved-domain search (18), the protein was called PhnF (36) (Fig. 1A). A search for TIGRFAM and Pfam matches for PhnF, using the search tools available via the TIGR website (http://cmr.tigr.org), revealed that the N terminus (amino acids 5 to 65) of the protein contained a helix-turn-helix motif of a GntR-like transcriptional regulator. The C-terminal part of the protein (amino acids 85 to 224) was a UbiC transcriptional regulator-associated (UTRA) domain, which is common to members of the HutC subfamily of GntR-like regulators and has been pro-

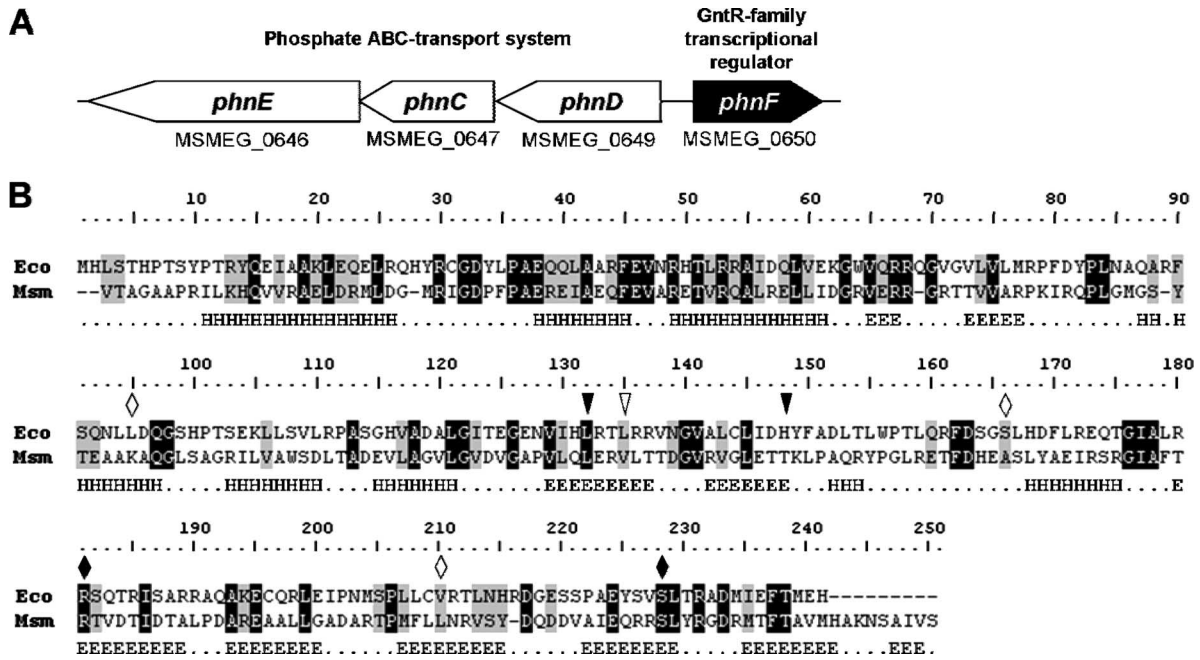

FIG. 1. Sequence analysis of *M. smegmatis* PhnF. (A) Map of the *phn* genes of *M. smegmatis*. The names of the loci, as annotated in the provisional genome sequence of *M. smegmatis* mc^2155, are indicated below the arrows. (B) Alignment of PhnF proteins from *E. coli* (Eco) and *M. smegmatis* (Msm). Identities are shown in black, and similarities (threshold, 90%) are shown in a gray background. The predicted secondary structure of *M. smegmatis* PhnF is shown below the sequence, with H indicating an α helix and E indicating a β sheet. Triangles indicate the large (L) and polar (H or T) signature residues of HutC subfamily proteins (2). Diamonds indicate the residues conserved among HutC members, which delineate the binding site of *E. coli* PhnF (8). Solid and open symbols show residues conserved and not conserved, respectively, in *M. smegmatis* PhnF.

posed to function in ligand binding (2). The predicted secondary structure of this region of *M. smegmatis* PhnF (Fig. 1B) showed a fold similar to the typical tandem arrangement of two α2-β-α-β2 repeats, further confirming that like the PhnF protein of *E. coli* (27), the *M. smegmatis* PhnF protein also belongs to the HutC subfamily. While few residues of the ligand binding pocket are conserved among members of this subfamily, two large residues in sheet 2 and one polar residue in sheet 3 appear to be universally conserved (2). An alignment between the *E. coli* and the *M. smegmatis* PhnF proteins shows that with the exception of Leu135 (*E. coli* numbering), these residues are conserved in the *M. smegmatis* protein (Fig. 1B). The crystal structure of *E. coli* PhnF showed that five residues conserved among PhnF orthologues delineate the proposed binding cavity (8). Only two of these residues (R181 and S228 [*E. coli* numbering]) are also conserved in the *M. smegmatis* protein (Fig. 1B). *E. coli* PhnF is thought to respond to the presence of alkylphosphonates (2, 8), but this seems unlikely to be the signal recognized by *M. smegmatis* PhnF, because the PhnDCE system does not appear to transport such compounds and because *M. smegmatis* cannot utilize phosphonates as phosphorous sources for growth (5). Differences in the signaling molecule recognized by the proteins from *E. coli* and *M. smegmatis* could explain the poor conservation of binding site residues between them. No *phnF* homologues have been identified in any of the other sequenced mycobacterial genomes, but a locus containing homologues to all four of the *phn* genes of *M. smegmatis* has been annotated in the genome of another actinomycete, *Nocardia farcinica* IFM 10152 (14).

The expression of *phnF* is induced by phosphate limitation. Both of the operons for the high-affinity phosphate transport systems identified in *M. smegmatis* to date, *phnDCE* and *pstSCAB*, are induced when the culture enters phosphate limitation at a threshold phosphate concentration of 40 μM (5). If PhnF had a role in the regulation of one or both of these operons, then it was conceivable that the expression of the *phnF* gene also responded to the concentration of phosphate in the growth medium. To test this hypothesis, we created a transcriptional fusion of the putative promoter area (ca. 500 bp) of *phnF* to that of *lacZ* (pSG18). An *M. smegmatis* strain carrying this construct was grown in a phosphate-limited minimal medium as described previously (5), and the phosphate concentration, the β-galactosidase activity, and the OD_{600} were monitored throughout growth. Activities of the *phnF-lacZ* fusion rapidly increased from between 25 and 40 MU under phosphate-replete conditions to approximately 150 MU when the phosphate concentration in the medium dropped to below 40 μM (Fig. 2). The expression of *phnF-lacZ* therefore followed the same expression pattern as that of *phnD-lacZ* and *pstS-lacZ*, even though the magnitude of induction (ca. 4-fold) was much smaller than those observed for *phnD* and *pstS* (26-fold and 17-fold, respectively) (5). These data strongly suggest that PhnF is involved in the adaptation of *M. smegmatis* to phosphate-limited conditions.

Construction of a *phnF* deletion mutant. To further elucidate the function of PhnF, we created a *phnF* deletion mutant by allelic exchange mutagenesis. A construct in which *phnF* was replaced with a kanamycin resistance cassette, *aphA-3*, was

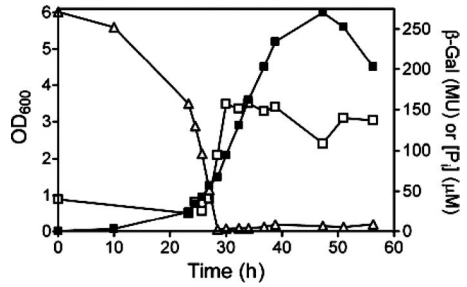

FIG. 2. Transcriptional activities of *phnF-lacZ* during phosphate-limited growth. Cells were grown in modified minimal Sauton's medium (5 g glycerol liter^{-1}, 4 g L-asparagine liter^{-1}, 200 μM P_i) and monitored for growth, expressed as OD_{600} (■), phosphate concentration in the medium (P_i) (△), and β-galactosidase activity (β-Gal), expressed as MU (□). Representative results of two independent experiments are shown.

cloned into pX33, as described in Materials and Methods, and *M. smegmatis* mc^{2}155 was transformed with the resulting plasmid. Knockout mutants were selected as described previously (26). The replacement of *phnF* with the antibiotic marker introduced two additional SmaI restriction sites, resulting in a band shift from 6.7 kb in the wild type to 3.2 kb in the deletion mutant (strain SG62) in Southern hybridization analysis of SmaI-digested genomic DNA probed with a radiolabeled PCR product of the left flank of the deletion construct (Fig. 3). For complementation, an integrative plasmid containing *phnF* plus ca. 500 bp of the region upstream of the predicted translational start site was introduced into strain SG62, creating strain SG111.

Deletion of *phnF* leads to the overexpression of *phnDCE* but not *pstSCAB*. In order to determine any of the effects that the deletion of *phnF* would have on the expression of the *phnDCE* and *pstSCAB* operons, we analyzed the relative amounts of mRNA synthesized by both of the operons in the wild type and the *phnF* deletion strain (SG62) under high- and low-phosphate conditions. In the wild-type strain, both of the *phnDCE* and *pstSCAB* operons were expressed at low levels in the high-phosphate samples, and expression was increased strongly in phosphate-starved cells (Fig. 4A), as was expected from previous results obtained from transcriptional *lacZ* fusion analyses (5). The deletion of *phnF* had no effect on the expression of the *pstSCAB* operon, which showed the same expression patterns in the SG62 Δ*phnF* strain, the SG111 complemented strain, and the wild-type strain (Fig. 4A, top panel). In contrast, the expression of *phnDCE* was strongly increased in the phosphate-starved cells of the *phnF* deletion mutant strain SG62 compared to that in the cells of the wild-type strain (Fig. 4A, bottom panel). The expression level of *phnDCE* under high-phosphate conditions was not changed in the SG62 strain. Complementation of the *phnF* deletion completely restored expression patterns to the wild-type level, confirming that the increase observed for expression under phosphate-starved conditions was indeed due to the deletion of *phnF*. These data clearly show that PhnF acts as a repressor of *phnDCE*. PhnF appears to have no role in the regulation of *pstSCAB*. The fact that the deletion of *phnF* does not lead to full constitutive expression of *phnDCE* under high-phosphate conditions suggests that a further regulatory mechanism is required for the induction of the operon. This hypothesis is addressed below.

Deletion of *pstS* leads to the constitutive expression of *pstSCAB*, *phnDCE*, and *phnF*. As mentioned above, the expression of the *phnDCE* operon appears to be subject to dual regulation: repression by PhnF and activation by a second regulatory mechanism. The most probable candidate for this second regulatory mechanism is the SenX3-RegX3 two-component system, which is reported to regulate the expression of the *pstSCAB* operon (6). SenX3, like its functional counterpart PhoR of *E. coli*, lacks any significant extracellular loops, which led to the proposal that the Pst system of *M. smegmatis* functions as the actual sensor of extracellular phosphate concentration (6). Accordingly, mutations in either *pstS*, *pstC*, or *pstA* are sufficient for the derepression of *phoA* expression (15), which is known to be under the control of SenX3-RegX3 (6). We therefore utilized the *M. smegmatis pstS* deletion mutant (strain SG95) and the *pstS*-complemented strain (SG120) (5) to determine whether the expression of *phnDCE* was affected by *pstS* deletion and thus was likely to be under the control of SenX3-RegX3. Using RNA dot blot analysis, a small but reproducible increase in the expression level of *phnDCE* was

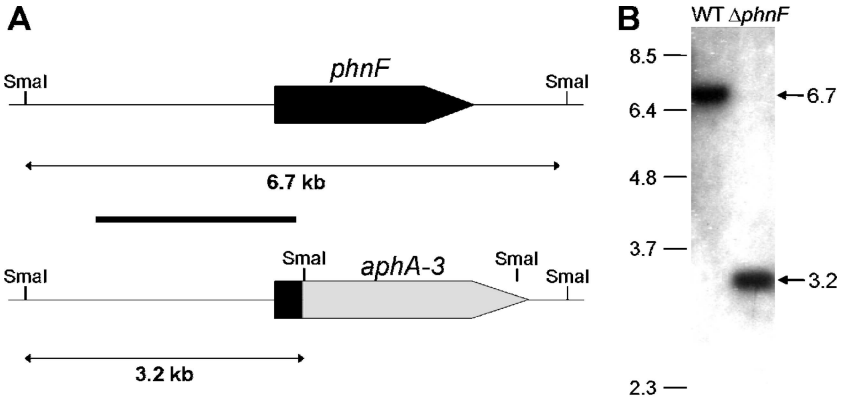

FIG. 3. Allelic replacement of *phnF*. (A) Schematic diagram (not drawn to scale) of allelic replacement of *phnF* with *aphA*-3. SmaI restriction sites and band sizes as detected in panel B are indicated. The bold line shows the fragment used as a probe. (B) Southern hybridization analysis of the replacement of *phnF* in strain SG62. SmaI-digested genomic DNA from the wild-type (WT) strain and from strain SG62 (Δ*phnF*) was probed with the radiolabeled left-flank PCR product of the deletion construct. Molecular sizes are indicated in kilobases.

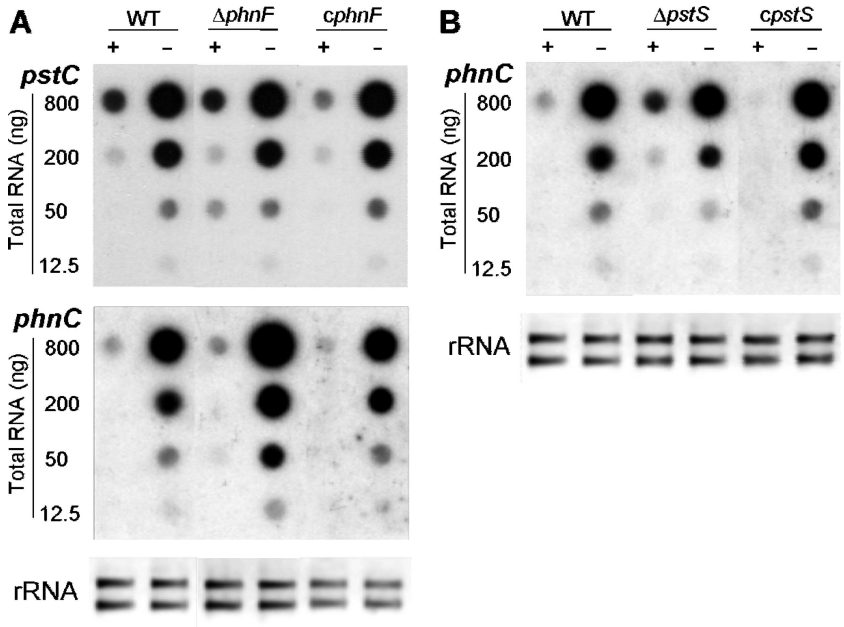

FIG. 4. Dot blot analysis of RNA from wild-type and mutant strains. Fourfold dilutions of total RNA isolated from cells grown in high-phosphate medium (100 mM; +) or subjected to phosphate starvation for 2 h (−) were spotted onto nylon membranes. Membranes were probed with radiolabeled PCR products from internal fragments of *pstC* (A, top panel) or *phnC* (A, bottom panel, and B). Amounts of total RNA per spot are shown in ng. Strains are indicated above the autoradiographs. (A) WT, wild-type; Δ*phnF*, *phnF* deletion strain SG62; c*phnF*, *phnF*-complemented strain SG111. (B) WT, wild-type; Δ*pstS*, *pstS* deletion strain SG95; c*pstS*, *pstS*-complemented strain SG120. Representative results of two to three independent experiments are shown. Below each panel, 16S and 23S rRNA bands from 300 ng total RNA per sample on an agarose gel stained with ethidium bromide are shown as controls. Lanes correspond to the samples in the rows above.

observed with the high-phosphate samples of strain SG95 (Δ*pstS*) compared to that in the wild-type strain, and no differences in the wild-type expression levels were observed with phosphate-starved cells (Fig. 4B). Complementation of the *pstS* deletion restored *phnDCE* expression to the wild-type pattern.

To study this pattern of gene expression in more detail, we introduced the transcriptional *phnD-lacZ* construct (pSG10) (5) into strain SG95 (Δ*pstS*) and monitored the expression patterns in both the phosphate-replete and the phosphate-starved cells. As a control, the transcriptional *pstS-lacZ* construct, pSG42 (5), was introduced into strain SG95 (Δ*pstS*), because the *pstS* promoter is known to be regulated by RegX3 (6) and thus should be constitutively expressed in a *pstS* deletion background. In cells of the wild-type strain carrying the *pstS-lacZ* construct pSG42, phosphate starvation led to a five- to sixfold increase in β-galactosidase activity, from ca. 10 MU to 55 MU, compared to that in cells grown under phosphate-replete conditions (Fig. 5A). Cells of the *pstS* deletion strain SG95 harboring *pstS-lacZ* had β-galactosidase activities of ca. 80 MU, independent of the phosphate concentration available. In the complemented strain SG120, regulation was restored, and phosphate starvation led to a fivefold induction of β-galactosidase activity, although the absolute levels of activity were lower than in the wild-type strain. These data show that the deletion of *pstS* causes constitutive expression from the RegX3-dependent *pst* promoter. Cells of the wild-type strain carrying the *phnD-lacZ* construct pSG10 displayed a 20-fold induction of β-galactosidase activity in response to phosphate starvation (Fig. 5B). In contrast, the expression of *phnD-lacZ* in SG95 (Δ*pstS*) was constitutive at around 100 MU. Complementation of the *pstS* deletion restored the regulation of expression to that of wild-type levels.

To study the effect of *pstS* deletion on *phnF* expression, *phnF-lacZ* activity was measured in the wild-type strain and in the SG95 strain (Δ*pstS*). In the wild-type strain carrying the *phnF-lacZ* construct, phosphate starvation led to a 2.6-fold induction, from 35 MU to 90 MU, while in strain SG95, the expression of *phnF-lacZ* was constitutive at about 80 MU (Fig. 5C). In the complemented strain SG120, β-galactosidase activity was lower than that in the wild-type strain, but phosphate starvation-dependent induction was restored to a 3-fold level.

These data demonstrate that *pstS* deletion leads to constitutive expression of *phnDCE* and *phnF* under phosphate-replete and phosphate-starved conditions. However, RNA analysis of *phnDCE* expression in phosphate-replete cells of the *pstS* deletion mutant indicated that the derepression was only partial. We attribute this discrepancy to the differences in copy numbers of the *phnDCE* promoter region in the two experiments: for RNA analysis, PhnF is able to exert its repressive effect on the single copy of the *phnDCE* promoter. In contrast, *phnD-lacZ* is present as 3 to 10 copies per cell (34), and therefore the effect of PhnF is titrated out. Taken together, these results show that the expression from the *phnDCE* and *phnF* promoters, like that from the *pstSCAB* promoter, is increased in a *pstS* deletion background. The *phnDCE* operon and *phnF* thus appear to be likely new candidates for the SenX3-RegX3 regulon of *M. smegmatis*, in which *phnDCE* is under additional control by the repressor PhnF. Further work is required to confirm the involvement of SenX3-RegX3 in the

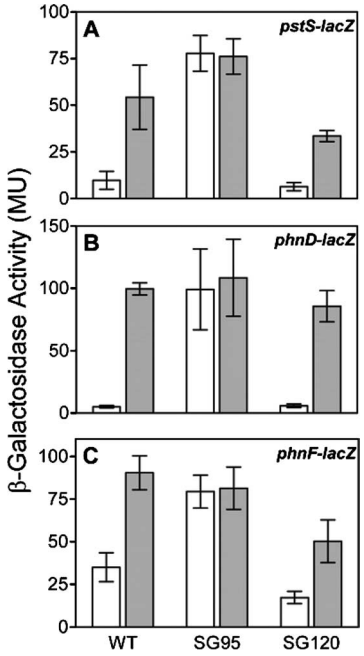

FIG. 5. Expression levels of *pstS-lacZ*, *phnD-lacZ*, and *phnF-lacZ* in various genetic backgrounds of *M. smegmatis*. Cells of the wild type (WT), the *pstS* deletion strain (SG95), and the complemented strain (SG120) carrying various *lacZ* fusion constructs were grown in ST medium containing 100 mM P_i (open bars) or subjected to phosphate starvation for 2 h (gray bars). β-Galactosidase activities are given as MU. (A) Cells harboring the pSG42 plasmid (*pstS-lacZ*). (B) Cells harboring the pSG10 plasmid (*phnD-lacZ*). (C) Cells harboring the pSG18 plasmid (*phnF-lacZ*). Results are shown as the means and standard deviations of results from two to four independent experiments. Differences between cells grown in 100 mM P_i and phosphate-starved cells of the wild-type and those of the SG120 strain and differences between the wild-type cells grown in 100 mM P_i and the cells of the SG95 strain are statistically significant ($P < 0.05$).

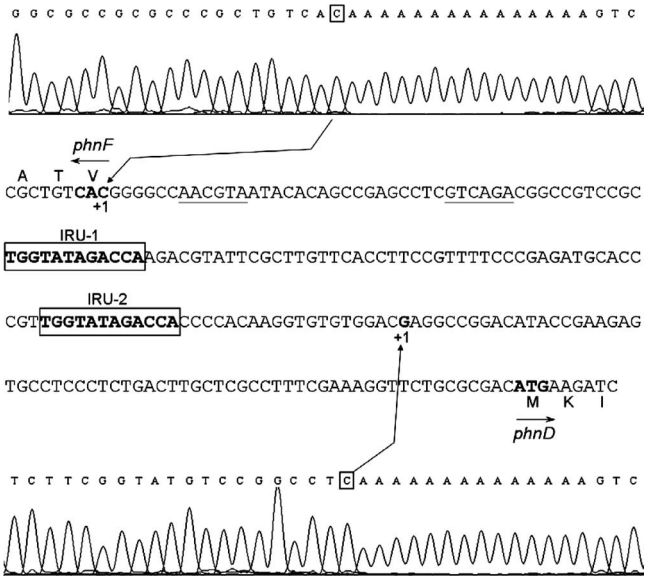

FIG. 6. Sequence analysis of the intergenic region between *phnF* and *phnD*. Transcriptional start sites for *phnF* and *phnD* were determined by 5′ RACE analysis as shown in the top and bottom panels, respectively (traces are given as reverse sequences). The sequence given in the middle panel shows a region of the coding strand for *phnD*, encompassing the first three codons of *phnF* and *phnD* (the first three amino acids are indicated) and the intergenic region. It should be noted that the sequence for *phnF* is therefore given as a reverse sequence. Start codons are shown in bold; transcriptional start sites are shown in bold and are indicated as +1. Putative −10 and −35 regions for *phnF* are underlined. The two IRUs, which constitute presumptive PhnF binding sites, are boxed.

regulation of *phnDCE* and *phnF* and whether there is direct interaction between RegX3 and these promoters.

The region between *phnF* and *phnD* contains two putative binding sites for PhnF. To gain further understanding of the involvement of the different transcription factors in the regulation of the *phnDCE* and *phnF* promoters, we determined the TSSs for both *phnD* and *phnF*, using 5′ RACE analysis (Fig. 6). The TSS for *phnD* was determined as the "G" located 65 bp upstream of the translational start. No consensus −10 or −35 sequences could be identified for *phnD*. The TSS for *phnF* was determined as the first nucleotide of the GTG start codon, suggesting that *phnF* is transcribed as a leaderless transcript, a feature which has also been observed for other GntR family transcriptional regulators from actinomycetes (12, 30). Putative −10 (5′-TACGTT-3′) and −35 (5′-TCTGAC-3′) boxes with some similarities to mycobacterial promoter elements (1, 29) could be identified upstream of the *phnF* TSS (Fig. 6).

Next, we searched both promoter regions for conserved binding motifs. RegX3 of *M. smegmatis* has been shown to bind to a loosely conserved inverted repeat (GTGAAC) separated by seven nucleotides in the promoters of *phoA*, *pstS*, and *senX3* (6). We analyzed 500-bp regions upstream of *phnD* and *phnF* but were unable to identify sequences with obvious similarity to the previously described RegX3 binding sites. Analysis of the same promoter areas, together with 500-bp regions with phosphate-responsive promoter activity for one of the *M. tuberculosis pst* operons (35), using a MEME motif discovery and search tool, also did not lead to the identification of potential RegX3 binding sites. It is likely that the number of mycobacterial genes known to respond to phosphate starvation is not yet large enough to identify common motifs in their promoter areas.

As discussed above, PhnF is a member of the HutC subfamily of GntR-like transcriptional regulators. A core recognition sequence for HutC-type regulators has been predicted (27), and more recently, the binding site of a member of this subfamily, DasR from *Streptomyces coelicolor*, has been identified as the 16-bp palindromic sequence ACTGGTCTACACCATT (28). Analysis of the intergenic region between *M. smegmatis phnD* and *phnF* revealed the presence of two inverted repeats with a similar sequence of TGGTATAGACCA, which we termed IRU-1 and IRU-2 (Fig. 6). The same sequence has recently been identified as a potential binding site for PhnF by an in silico analysis of the *M. smegmatis* GntR family regulators (38).

To further investigate the role of IRU-1 and IRU-2, we introduced site-directed changes on a 377-bp PCR product encompassing the 199-bp intergenic region between *phnF* and *phnD* plus 93 bp of the start of the *phnF* coding region and 85 bp of the start of the *phnD* coding region. IRU-1 was changed to TGTGATAGACAC (mutated nucleotides are underlined), changing the sequence of each half site as well as the palin-

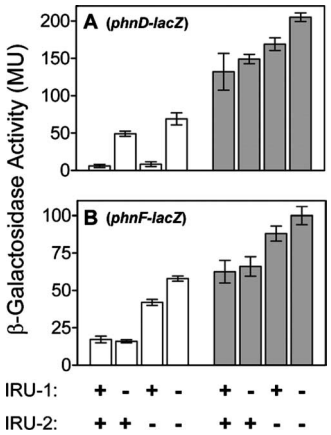

FIG. 7. Effects of site-directed mutagenesis of the IRUs in the intergenic region between *phnF* and *phnD* on gene expression. Changes were introduced into IRU-1 and IRU-2 (see text for details), and effects were monitored as the expression of *phnD-lacZ* (A) and *phnF-lacZ* (B) transcriptional fusions. Cells were grown in minimal Sauton's medium containing 100 mM phosphate (open bars) or starved in phosphate-free medium for 2 h (gray bars). The presence of wild-type sequences (+) or site-directed changes (−) in each IRU are shown below the graphs. Results are shown as the means and standard deviations from three independent experiments.

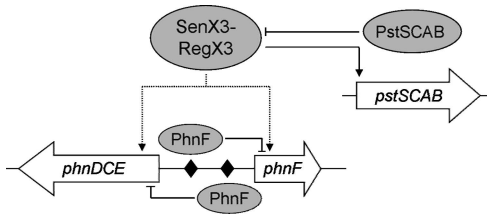

FIG. 8. Model for the regulation of *pstSCAB*, *phnDCE*, and *phnF* in *M. smegmatis*. Genes are shown as open arrows; proteins are shown as gray ovals. Flat-headed arrows indicate negative regulation; a pointed arrowhead indicates positive regulation. Dotted lines indicate that the proposed regulation may be direct or indirect. The presumptive PhnF binding sites are shown as black diamonds.

dromic structure. The 5′ half of IRU-2 reaches to nucleotide −31 relative to the *phnD* TSS. To avoid introducing changes into a region that might function as a −35 element of the *phnD* promoter, this part of the IRU-2 was therefore left unchanged, leading to a mutated sequence of TGGTATACCACA. A third fragment containing the changes in both regions was amplified. The three mutated fragments as well as a PCR product containing the wild-type sequence were then used to construct transcriptional *lacZ* fusions of either the *phnF* or the *phnDCE* promoters, depending on the orientation of the insert. The effect of the mutations on promoter activity were then determined with cells grown under phosphate-replete conditions (100 mM phosphate in minimal Sauton's medium) and after 2 h of phosphate starvation. β-Galactosidase activities in cells carrying constructs with the wild-type sequence were comparable to the results obtained previously for the *phnF-lacZ* and *phnD-lacZ* constructs, in which phosphate starvation led to ca. 20-fold induction for the *phnD-lacZ* construct (Fig. 7A) and 3- to 4-fold induction for the *phnF-lacZ* construct (Fig. 7B). We therefore concluded that the fragment used for site-directed mutagenesis was sufficient for the phosphate-dependent control of *phnDCE* and *phnF* expression. The mutation of IRU-1 led to a partial but significant ($P < 0.0001$) derepression (an 8-fold increase compared to that of the wild-type promoter) of the *phnDCE* promoter under phosphate-replete conditions (Fig. 7A). Phosphate starvation further induced expression by approximately 2.7-fold ($P < 0.0001$). The mutation of IRU-2 had no significant effect on the expression of the *phnDCE* promoter. The mutation of both putative binding sites simultaneously increased the expression of the *phnDCE* promoter even further than the mutation of IRU-1 alone, under both phosphate-replete and phosphate-starved conditions ($P < 0.01$). The expression of *phnF* was unaffected by the mutation of IRU-1, whereas the mutation of IRU-2 led to a 2.5-fold increase in β-galactosidase activity under phosphate-replete conditions compared to that of the wild-type promoter ($P < 0.0001$) (Fig. 7B). Phosphate starvation still led to a twofold induction of expression ($P = 0.0001$). As observed for the *phnDCE* expression level, the mutation of both IRU-1 and IRU-2 simultaneously further increased the expression of *phnF* under both conditions tested ($P < 0.05$). These data suggest that IRU-1 is required for the repression of *phnDCE* transcription, while IRU-2 is required to repress the transcription of *phnF*. IRU-1 is centered at position −83.5 relative to the *phnD* TSS. IRU-2 is centered at position −110.5 relative to the *phnF* TSS. It is likely that IRU-1 and IRU-2 are binding sites for PhnF, and *phnF* would therefore appear to be subject to autoregulation.

Conclusions. In the present study, we investigated the transcriptional regulation of two operons, *pstSCAB* and *phnDCE*, encoding high-affinity phosphate transport systems of *M. smegmatis*. We showed that the *phn* locus contains another gene, *phnF*, which encodes a functional transcriptional regulator belonging to the HutC subfamily of GntR-like regulators. Furthermore, we demonstrated that PhnF acts as a repressor of the *phnDCE* operon but does not affect the expression of *pstSCAB*. Two presumptive binding sites for PhnF were identified in the region between *phnD* and *phnF*, and these sites are required for the repression of *phnD* and *phnF*. The deletion of *pstS* leads to the constitutive expression of *phnDCE* and *phnF*, suggesting that these genes may be under the control, directly or indirectly, of the SenX3-RegX3 system of *M. smegmatis*.

Based on these findings, we propose a model for the regulation of the *phnDCE* and *pstSCAB* operons in *M. smegmatis* (Fig. 8). Both operons are strongly induced by phosphate limitation. The *pstSCAB* operon is under the sole and direct control of SenX3-RegX3. In contrast, *phnDCE* expression at a low-phosphate concentration requires both the derepression by PhnF and the activation by a second system, presumably SenX3-RegX3. Transcription of *phnF* also appears to be under such dual control of activation by SenX3-RegX3 and repression by PhnF itself. Increased expression of PhnF under phosphate-limited conditions may supply the cell with a means to reestablish the repression of the Phn system when phosphate availability improves. Such a phenomenon of induction of repressors for the Pho regulon, *pstSCAB* and *phoU*, has been reported for *E. coli* and seems to be required to terminate the phosphate starvation response (39). Further work is required to determine whether PhnF and RegX3 interact directly with

the promoters studied here or indirectly via additional regulatory systems and to study how these different regulatory proteins interact with each other or with RNA polymerase. The differences in regulation between the Pst and Phn systems of *M. smegmatis* described here may shed light on the differences between the multiple phosphate transport systems present in other mycobacterial species. It has been proposed previously that the requirement of several such systems by mycobacteria may reflect subtle adaptations of the bacteria to a highly variable environment (17). In this case, the differential regulation of gene expression, as observed here, may be a key feature of mycobacterial phosphate transport systems.

ACKNOWLEDGMENTS

This work was funded by a New Zealand Lottery health grant. S.G. was supported by a University of Otago Prestigious Postgraduate Scholarship.

We thank Vernon Ward for helpful advice regarding the 5′ RACE experiments. We also thank Desmond Collins for supplying the pUHA267 plasmid.

REFERENCES

1. **Agarwal, N., and A. K. Tyagi.** 2006. Mycobacterial transcriptional signals: requirements for recognition by RNA polymerase and optimal transcriptional activity. Nucleic Acids Res. **34:**4245–4257.
2. **Aravind, L., and V. Anantharaman.** 2003. HutC/FarR-like bacterial transcription factors of the GntR family contain a small molecule-binding domain of the chorismate lyase fold. FEMS Microbiol. Lett. **222:**17–23.
3. **Bardin, S., S. Dan, M. Osteras, and T. M. Finan.** 1996. A phosphate transport system is required for symbiotic nitrogen fixation by *Rhizobium meliloti*. J. Bacteriol. **178:**4540–4547.
4. **Cuff, J. A., M. E. Clamp, A. S. Siddiqui, M. Finlay, and G. J. Barton.** 1998. JPred: a consensus secondary structure prediction server. Bioinformatics **14:**892–893.
5. **Gebhard, S., S. L. Tran, and G. M. Cook.** 2006. The Phn system of *Mycobacterium smegmatis*: a second high-affinity ABC-transporter for phosphate. Microbiology **152:**3453–3465.
6. **Glover, R. T., J. Kriakov, S. J. Garforth, A. D. Baughn, and W. R. Jacobs, Jr.** 2007. The two-component regulatory system *senX3-regX3* regulates phosphate-dependent gene expression in *Mycobacterium smegmatis*. J. Bacteriol. **189:**5495–5503.
7. **Gonzalez-y-Merchand, J. A., I. Estrada-Garcia, M. J. Colston, and R. A. Cox.** 1996. A novel method for the isolation of mycobacterial DNA. FEMS Microbiol. Lett. **135:**71–77.
8. **Gorelik, M., V. V. Lunin, T. Skarina, and A. Savchenko.** 2006. Structural characterization of GntR/HutC family signaling domain. Protein Sci. **15:** 1506–1511.
9. **Hall, T. A.** 1999. BioEdit: a user-friendly biological sequence alignment editor and analysis program for Windows 95/98/NT. Nucleic Acids Symp. Ser. **41:**95–98.
10. **Hanahan, D., J. Jessee, and F. R. Bloom.** 1991. Plasmid transformation of *Escherichia coli* and other bacteria. Methods Enzymol. **204:**63–113.
11. **Ho, S. N., H. D. Hunt, R. M. Horton, J. K. Pullen, and L. R. Pease.** 1989. Site-directed mutagenesis by overlap extension using the polymerase chain reaction. Gene **77:**51–59.
12. **Hoskisson, P. A., S. Rigali, K. Fowler, K. C. Findlay, and M. J. Buttner.** 2006. DevA, a GntR-like transcriptional regulator required for development in *Streptomyces coelicolor*. J. Bacteriol. **188:**5014–5023.
13. **Hulett, F. M.** 1995. Complex phosphate regulation by sequential switches in *Bacillus subtilis*, p. 298–302. *In* J. A. Hoch and T. J. Silhavy (ed.), Two-component signal transduction. American Society for Microbiology, Washington, DC.
14. **Ishikawa, J., A. Yamashita, Y. Mikami, Y. Hoshino, H. Kurita, K. Hotta, T. Shiba, and M. Hattori.** 2004. The complete genomic sequence of *Nocardia farcinica* IFM 10152. Proc. Natl. Acad. Sci. USA **101:**14925–14930.
15. **Kriakov, J., S. Lee, and W. R. Jacobs, Jr.** 2003. Identification of a regulated alkaline phosphatase, a cell surface-associated lipoprotein, in *Mycobacterium smegmatis*. J. Bacteriol. **185:**4983–4991.
16. **Lee, M. H., L. Pascopella, W. R. Jacobs, Jr., and G. F. Hatfull.** 1991. Site-specific integration of mycobacteriophage L5: integration-proficient vectors for *Mycobacterium smegmatis*, *Mycobacterium tuberculosis*, and bacille Calmette-Guerin. Proc. Natl. Acad. Sci. USA **88:**3111–3115.
17. **Lefèvre, P., M. Braibant, L. de Wit, M. Kalai, D. Roeper, J. Grotzinger, J. P. Delville, P. Peirs, J. Ooms, K. Huygen, and J. Content.** 1997. Three different putative phosphate transport receptors are encoded by the *Mycobacterium tuberculosis* genome and are present at the surface of *Mycobacterium bovis* BCG. J. Bacteriol. **179:**2900–2906.
18. **Marchler-Bauer, A., and S. H. Bryant.** 2004. CD-search: protein domain annotations on the fly. Nucleic Acids Res. **32:**W327–W331.
19. **Ménard, R., P. J. Sansonetti, and C. Parsot.** 1993. Nonpolar mutagenesis of the *ipa* genes defines IpaB, IpaC, and IpaD as effectors of *Shigella flexneri* entry into epithelial cells. J. Bacteriol. **175:**5899–5906.
20. **Metcalf, W. W., and B. L. Wanner.** 1991. Involvement of the *Escherichia coli phn* (*psiD*) gene cluster in assimilation of phosphorus in the form of phosphonates, phosphite, P_i esters, and P_i. J. Bacteriol. **173:**587–600.
21. **Metcalf, W. W., and B. L. Wanner.** 1993. Mutational analysis of an *Escherichia coli* fourteen-gene operon for phosphonate degradation, using Tn*phoA′* elements. J. Bacteriol. **175:**3430–3442.
22. **Metcalf, W. W., and R. S. Wolfe.** 1998. Molecular genetic analysis of phosphite and hypophosphite oxidation by *Pseudomonas stutzeri* WM88. J. Bacteriol. **180:**5547–5558.
23. **Miller, J. H.** 1972. Experiments in molecular genetics. Cold Spring Harbor Laboratory Press, Cold Spring Harbor, NY.
24. **Monk, B. C., M. B. Kurtz, J. A. Marrinan, and D. S. Perlin.** 1991. Cloning and characterization of the plasma membrane H^+-ATPase from *Candida albicans*. J. Bacteriol. **173:**6826–6836.
25. **Peirs, P., P. Lefèvre, S. Boarbi, X. M. Wang, O. Denis, M. Braibant, K. Pethe, C. Locht, K. Huygen, and J. Content.** 2005. *Mycobacterium tuberculosis* with disruption in genes encoding the phosphate binding proteins PstS1 and PstS2 is deficient in phosphate uptake and demonstrates reduced in vivo virulence. Infect. Immun. **73:**1898–1902.
26. **Pelicic, V., M. Jackson, J. M. Reyrat, W. R. Jacobs, Jr., B. Gicquel, and C. Guilhot.** 1997. Efficient allelic exchange and transposon mutagenesis in *Mycobacterium tuberculosis*. Proc. Natl. Acad. Sci. USA **94:**10955–10960.
27. **Rigali, S., A. Derouaux, F. Giannotta, and J. Dusart.** 2002. Subdivision of the helix-turn-helix GntR family of bacterial regulators in the FadR, HutC, MocR, and YtrA subfamilies. J. Biol. Chem. **277:**12507–12515.
28. **Rigali, S., M. Schlicht, P. Hoskisson, H. Nothaft, M. Merzbacher, B. Joris, and F. Titgemeyer.** 2004. Extending the classification of bacterial transcription factors beyond the helix-turn-helix motif as an alternative approach to discover new *cis*/*trans* relationships. Nucleic Acids Res. **32:**3418–3426.
29. **Rodrigue, S., J. Brodeur, P. E. Jacques, A. L. Gervais, R. Brzezinski, and L. Gaudreau.** 2007. Identification of mycobacterial σ factor binding sites by chromatin immunoprecipitation assays. J. Bacteriol. **189:**1505–1513.
30. **Ryding, N. J., G. H. Kelemen, C. A. Whatling, K. Flardh, M. J. Buttner, and K. F. Chater.** 1998. A developmentally regulated gene encoding a repressor-like protein is essential for sporulation in *Streptomyces coelicolor* A3(2). Mol. Microbiol. **29:**343–357.
31. **Sambrook, J., E. F. Fritsch, and T. Maniatis.** 1989. Molecular cloning: a laboratory manual, 2nd ed. Cold Spring Harbor Laboratory Press, Cold Spring Harbor, NY.
32. **Snapper, S. B., R. E. Melton, S. Mustafa, T. Kieser, and W. R. Jacobs, Jr.** 1990. Isolation and characterization of efficient plasmid transformation mutants of *Mycobacterium smegmatis*. Mol. Microbiol. **4:**1911–1919.
33. **Sola-Landa, A., A. Rodriguez-Garcia, E. Franco-Dominguez, and J. F. Martin.** 2005. Binding of PhoP to promoters of phosphate-regulated genes in *Streptomyces coelicolor*: identification of PHO boxes. Mol. Microbiol. **56:** 1373–1385.
34. **Timm, J., E. M. Lim, and B. Gicquel.** 1994. *Escherichia coli*-mycobacteria shuttle vectors for operon and gene fusions to *lacZ*: the pJEM series. J. Bacteriol. **176:**6749–6753.
35. **Torres, A., M. D. Juarez, R. Cervantes, and C. Espitia.** 2001. Molecular analysis of *Mycobacterium tuberculosis* phosphate specific transport system in *Mycobacterium smegmatis*. Characterization of recombinant 38 kDa (PstS-1). Microb. Pathog. **30:**289–297.
36. **Tran, S. L., M. Rao, C. Simmers, S. Gebhard, K. Olsson, and G. M. Cook.** 2005. Mutants of *Mycobacterium smegmatis* unable to grow at acidic pH in the presence of the protonophore carbonyl cyanide m-chlorophenylhydrazone. Microbiology **151:**665–672.
37. **van Veen, H. W.** 1997. Phosphate transport in prokaryotes: molecules, mediators and mechanisms. Antonie van Leeuwenhoek **72:**299–315.
38. **Vindal, V., K. Suma, and A. Ranjan.** 2007. GntR family of regulators in *Mycobacterium smegmatis*: a sequence and structure based characterization. BMC Genomics **8:**289.
39. **Wanner, B. L.** 1996. Phosphorus assimilation and control of the phosphate regulon, p. 1357–1381. *In* F. C. Neidhardt, R. Curtiss III, J. L. Ingraham, E. C. C. Lin, K. B. Low, B. Magasanik, W. S. Reznikoff, M. Riley, M. Schaechter, and H. E. Umbarger (ed.), *Escherichia coli* and *Salmonella*: cellular and molecular biology, 2nd ed., vol. 1. ASM Press, Washington, DC.
40. **White, A. K., and W. W. Metcalf.** 2004. Two C-P lyase operons in *Pseudomonas stutzeri* and their roles in the oxidation of phosphonates, phosphite, and hypophosphite. J. Bacteriol. **186:**4730–4739.
41. **Yuan, Z. C., R. Zaheer, and T. M. Finan.** 2006. Regulation and properties of PstSCAB, a high-affinity, high-velocity phosphate transport system of *Sinorhizobium meliloti*. J. Bacteriol. **188:**1089–1102.